

Intracavity optical pumping of J-aggregate microcavity exciton polaritons

M. Scott Bradley and Vladimir Bulović*

Organic and Nanostructured Electronics Laboratory, Center for Excitonics, Massachusetts Institute of Technology, Cambridge, Massachusetts 02139, USA

(Received 30 March 2010; revised manuscript received 23 June 2010; published 29 July 2010)

We demonstrate intracavity optical pumping of J-aggregate microcavity exciton polaritons. The use of ultrathin layer-by-layer J-aggregate thin films as the strongly coupled exciton medium allows for inclusion of a thermally evaporated luminescent cavity spacer layer, through which the lower-branch exciton-polariton states are resonantly pumped. We present a measurement of the lower-branch exciton-polariton occupation in room-temperature microcavity devices containing J-aggregated molecular thin films under low-density steady-state excitation. The observed exciton-polariton occupation shows a Maxwell-Boltzmann distribution at $T = 300$ K, indicating thermalization of exciton polaritons in the lower energy branch. This device design enables us to propose a new type of “polariton laser” architecture for microcavity exciton polaritons.

DOI: [10.1103/PhysRevB.82.033305](https://doi.org/10.1103/PhysRevB.82.033305)

PACS number(s): 78.55.Kz, 71.36.+c, 81.05.Fb

Microcavity structures containing organic thin films can manifest strong coupling of light and matter even at room-temperature conditions due to the large oscillator strength and high-binding energy of the Frenkel exciton transitions in organic molecular thin films.^{1–4} The ease of incorporating room-temperature-deposited layered organic materials into microcavity devices enabled the first demonstration of electroluminescence of microcavity exciton polaritons from an organic light-emitting device containing a thin film of the strongly coupled organic material.⁵ Inorganic exciton-polariton devices have been used to demonstrate coherent light emission from optically pumped lower-branch exciton-polariton states,^{6–9} which may be a first indication of the superfluidity that has been theoretically predicted for microcavity exciton polaritons. Such polariton lasing was recently demonstrated in an organic exciton-polariton system, where microcavity photons were strongly coupled to crystalline anthracene.¹⁰ In both inorganic and organic systems, populating the lower-branch exciton polariton from uncoupled excitons (the “exciton reservoir”) is a challenge.^{11–13} The present study introduces a method of populating lower-branch J-aggregate microcavity exciton polaritons via intracavity optical pumping from an organic dye-doped luminescent spacer layer. At low-optical-pumping intensities the measured occupation of exciton polaritons in the lower-branch fits a Maxwell-Boltzmann distribution at $T = 300$ K, indicating that the polariton population is thermalized. We suggest a novel means of achieving polariton lasing in exciton-polariton devices and examine current literature on expected thresholds in organic exciton-polariton lasers.

Considerable theoretical research has examined the nature of exciton polaritons in both crystalline and disordered organic microcavities.^{14–17} One key result of this research is that exciton polaritons near $k_{\parallel} = 0$ in the lower polariton branch in organic systems are localized due to resonant scattering and structural inhomogeneities, similar to the disorder-induced localization of polaritons in GaN quantum-well systems.^{18,19} One of the effects of localization is that only a subset of excitonic states are strongly coupled to the normal mode of the microcavity, and population of the lower-branch exciton polaritons from uncoupled excitons via phonon-assisted scattering is limited.^{20–23} In the recently reported

result of polariton lasing in crystalline anthracene microcavities, the authors attribute sufficient population of the lower branch to photoluminescence from uncoupled excitons in anthracene, a pathway, which has recently been theoretically studied.^{10,24} Based on these earlier results, we suggest that J-aggregate microcavities, specifically with thin films of J-aggregates grown through the layer-by-layer (LBL) method, allow for deliberate intracavity optical pumping of lower-branch exciton-polariton states through the use of a luminescent cavity spacer layer.

The structure of devices measured in this study is shown in Fig. 1(a). A microcavity is formed using two distributed Bragg reflectors (DBRs) consisting of alternating pairs of layers of silicon dioxide (SiO_2) and titanium dioxide (TiO_2). The bottom, 14.5-pair $\text{TiO}_2/\text{SiO}_2$ DBR was commercially obtained from Visimax Technologies and was deposited via plasma-enhanced evaporation. The top, 10-pair $\text{TiO}_2/\text{SiO}_2$ DBR was deposited using automated radio-frequency sputtering; the TiO_2 was deposited in pure argon plasma, and the SiO_2 was deposited in argon plasma with 15% oxygen. The bottom cavity spacer is a sputter-deposited SiO_2 layer, (128.4 ± 0.3) nm thick (measured on a Gaertner ellipsometer), deposited using the same conditions as the SiO_2 layers in the top DBR. The J-aggregate thin film is deposited through spin self-assembly (SSA) of alternating layers of PDAC [poly(diallyldimethylammonium chloride), MW 4×10^5 , obtained from Sigma Aldrich, CAS 26062–79–3] and THIATS [Benzothiazolium, 5-chloro-2-[2-[[5-chloro-3-(3-sulfopropyl)-2(3H)-benzothiazolylidene]methyl]-1-buten-1-yl]-3-(3-sulfopropyl)-, inner salt, compounded with N,N-diethylethanamine (1:1) obtained from H.W. Sands, CAS 23568–98–1]. The THIATS solution used in the SSA process had a concentration of 100 μM in deionized (DI) water, made by diluting a 2 mg/mL stock solution in DI water. The PDAC solution was 3 mM in DI water.

SSA of polyelectrolyte thin films was first introduced in the early 2000s and has been utilized to make both thin films comprised of all polyelectrolytes and thin films of polyelectrolytes and oppositely charged particles (quantum dots, molecules, etc.).^{25–28} The process is similar to the LBL process in theory of operation, where oppositely charged layers are sequentially adsorbed with the excess loosely bound material

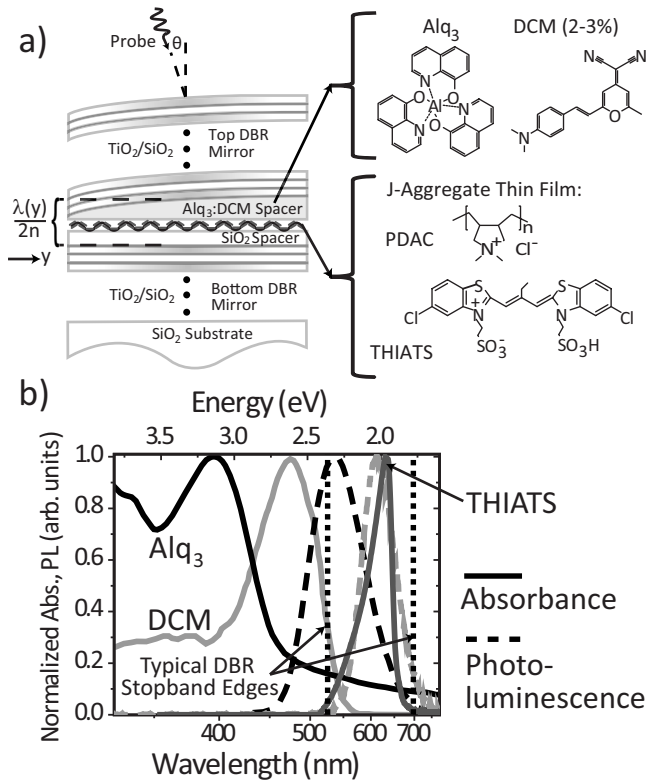


FIG. 1. (a) Graded-thickness microcavity device structure and molecular diagrams of constituent thin film materials. (b) Normalized absorbance (Abs) and photoluminescence (PL) spectra of Alq₃, DCM, and THIATS J-aggregates showing spectral overlaps governing energy down conversion from Alq₃ through DCM to THIATS J-aggregates.

rinsed, allowing for nanoscale thickness precision for deposited films. In LBL, the substrates are immersed in growth and rinse solutions, whereas in SSA, these solutions are poured on the substrate, followed by spinning of the substrate to dry. For growing only a few thin film samples, SSA is faster than a comparable LBL process and prevents cross-contamination of growth solutions. A hybrid process of SSA and a few LBL immersion steps can also be performed to allow deposition of J-aggregate thin films using less-water-soluble dyes than THIATS, such as TDBC, the J-aggregating dye used in the electroluminescence studies referenced above.^{5,29}

After the J-aggregate thin film is deposited on top of the bottom DBR, a luminescent top cavity spacer of varying thickness is thermally evaporated, consisting of Alq₃ [aluminum tris(8-hydroxyquinoline)] doped at 2% to 3% by weight with the laser dye DCM [4-(dicyanomethylene)-2-methyl-6-(4-dimethylaminostyryl)-4H-pyran]. The varying thickness of the spacer layer across the substrate [as sketched in Fig. 1(a)] is achieved by evaporating the Alq₃:DCM thin film through a fixed shadow mask onto a rotating substrate. The use of a luminescent Alq₃:DCM top cavity spacer allows for intracavity pumping of the THIATS J-aggregate microcavity exciton polaritons, as shown by the absorption and PL spectra of the various materials in the microcavity in Fig. 1(b). For PL measurements, the samples are pumped using a 4 mW $\lambda=408$ nm CW laser focused into a $a < 100$ μm diam-

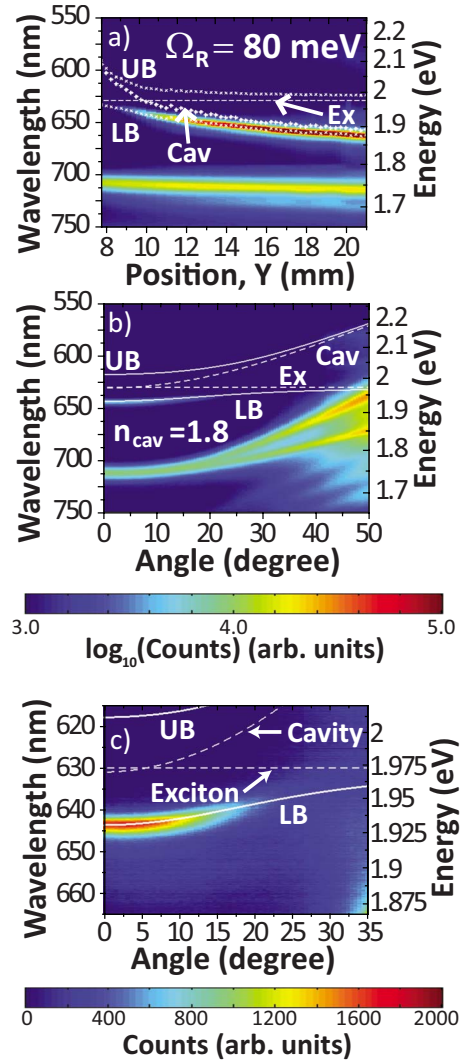


FIG. 2. (Color online) (a) PL spectrum versus position on sample with energies of lower-branch (LB) and upper-branch (UB) exciton-polariton modes, uncoupled cavity mode found with numerical fit (Cav), and uncoupled J-aggregate exciton (Ex). (b) PL spectrum versus angle at position $Y \sim 10$ mm on sample using low-resolution grating. (c) PL spectrum versus angle at same position as in (b) using high-resolution grating.

eter spot, which excites the Alq₃ and subsequently DCM through Förster transfer; the DCM then excites the THIATS exciton and exciton-polariton states through direct Förster transfer or through absorption of DCM PL by THIATS, depending on the proximity of the excited DCM molecules to the THIATS J-aggregate thin film. Angle-resolved PL is collected using a multimode optical fiber mounted on a custom-built automated rotation stage with $< 0.5^\circ$ resolution. The excitation laser strikes the sample at a 45° incident angle; a slight downward tilt to the optic axis is used to avoid collection of the reflected excitation beam by the fiber.

Figure 2 shows the PL intensity collected from the sample shown in Fig. 1(a) as a function of position on the sample surface, with the PL collected at normal incidence (i.e., $k_{\parallel} = 0$) [Fig. 2(a)] and as a function of angle of light collection away from the normal [Fig. 2(b) and 2(c)]. The exciton reso-

nance (i.e., the ground state to one-exciton transition of the J-aggregate) is assumed to be at a free-space wavelength of $\lambda_{J-Agg}=630$ nm. The wavelength of the cavity resonance, λ_{cav} , is calculated at each position by fitting the observed peak in the lower-branch exciton-polariton PL to that predicted by the coupled light and two-level system eigenenergy equation:

$$E_{\pm} = \frac{1}{2}(E_{cav} + E_{J-Agg}) \pm \frac{1}{2}\sqrt{\hbar^2\Omega_R^2 + (E_{cav} - E_{J-Agg})^2}, \quad (1)$$

where $E_{+/-}$ are the upper and lower-branch exciton-polariton eigenenergies, E_{cav} is the energy of the cavity resonance corresponding to $\lambda_{cav}=hc/E_{cav}$, E_{J-Agg} is the exciton resonance corresponding to the λ_{J-Agg} , and $\hbar\Omega_R$ is the Rabi splitting, with $\hbar\Omega_R=80$ meV used for the fit.

Figure 2(b) shows the angle-resolved PL at nearly-zero detuning [position $Y \sim 10$ mm on the Fig. 2(a) plot]. Note that the PL intensity in this figure is plotted on a logarithmic color chart, as indicated. Replacing E_{cav} in Eq. (1) with the angle-dependent cavity resonance given by

$$E_{cav}(\theta) = \frac{E_{cav}(0^\circ)}{\sqrt{1 - \frac{\sin^2 \theta}{n_{eff}^2}}}, \quad (2)$$

with θ corresponding to the light-emission angle away from the sample normal, we can fit the angular dispersion of the lower-branch exciton-polariton PL peak, finding the effective index of refraction of the cavity to be $n_{eff}=1.8$. Note that luminescence of DCM via the low-energy DBR Bragg modes in the wavelength range of $\lambda=650$ nm to $\lambda=725$ nm is also visible in the measured PL in Fig. 2(b), and at large angles the intensity increases due to the collection of waveguided emission in the far-field optical setup. Figure 2(c) plots the lower-branch exciton-polariton PL measured using a spectrometer grating with ~ 0.05 nm wavelength resolution on a more limited set of angles to avoid collecting waveguided emission, with the PL intensity plotted on a linear color chart, as indicated.

The measured intensity of the lower-branch exciton-polariton PL, shown in Fig. 2(c), is converted to a relative occupation number of the corresponding exciton-polariton states by taking account of both the effect of the multilayer planar structure on the observed emission intensity and the effect of the changing composition of the exciton polariton from photon to exciton due to the larger positive detuning of the cavity resonance from the exciton resonance as the emission angle increases. The former is an effect of Snell's law and is corrected by dividing the observed counts by the cosine of the observation angle (as in Lambert's Cosine Law).¹² The latter is corrected by calculating the Hopfield coefficients at each angle and then dividing the observed counts at each angle by the respective photon fraction.³⁰ Figure 3(a) shows the observed counts of the lower-branch exciton-polariton PL (scaled to correct for the above effects) together with a superimposed plot of the Maxwell-Boltzmann (M-B) distribution at $T=300$ K. Figure 3(b) shows the photon and exciton fraction of the lower-branch calculated from the Hopfield coefficients and used in the scaling of the counts in

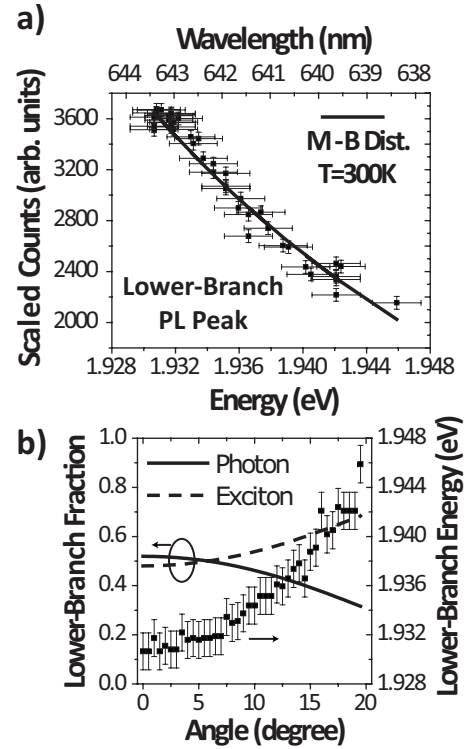


FIG. 3. (a) Relative lower branch exciton-polariton occupation indicated by scaled PL counts versus energy. PL counts are scaled by photon fraction versus angle and account for change in observed internal solid angle as the measurement angle changes. The solid line is a Maxwell-Boltzmann distribution at $T=300$ K. (b) Calculated photon and exciton fractions of the lower-branch exciton polariton versus angle along with energy of the peak in lower-branch PL versus angle.

Fig. 3(a). The good agreement between the measured lower-branch exciton-polariton relative occupation and the M-B distribution at $T=300$ K indicates that the exciton polaritons pumped into the lower-branch have thermalized prior to decay.

Use of the optically pumped luminescent spacer layer to inject exciton polaritons into the strongly coupled microcavity, which is then followed by the exciton-polariton thermalization in the lower branch, suggests a device architecture for a “polariton laser.” With sufficiently high reflectance of the microcavity mirrors, and a sufficient thickness of the luminescent cavity spacer gain material, the spacer material could undergo lasing in an exciton-polariton mode.

Although exciton-polariton lasers are generally expected to have a lower threshold than traditional vertical-cavity surface-emitting lasers (VCSELs), based on current literature, a comparison of the expected threshold of an organic VCSEL to that of an organic exciton-polariton laser is complicated by the lack of studies specific to organic exciton-polariton systems. Litinskaya *et al.* estimated a low threshold for organic exciton-polariton lasing relative to organic VCSELs by using the density of states of a planar microcavity to determine occupation threshold, but not accounting for the effect of dephasing on condensation, which has been studied at length in inorganic systems.^{31,32} From the literature on inorganic exciton-polariton systems, one might com-

pare GaN-quantum-well systems to organic systems since both are operated at room temperature and have similar Rabi splittings (30–150 meV) and exciton linewidths (15–50 meV),^{33,34} but some important distinctions remain. For example, the threshold of a quantum-well GaN-based exciton-polariton system, recently predicted theoretically, was 3×10^{12} excitations per cm^2 , which corresponds to one exciton polariton per $5.7 \times 5.7 \text{ nm}^2$.³⁵ Such a length scale is comparable to the Förster radius for molecule-to-molecule exciton energy transfer and to the exciton diffusion length of many molecular organic thin films, especially those with considerable spectral overlap of emission and absorption which are typically used in exciton-polariton devices. This proximity in length scale necessitates that dipole-dipole interactions, such as present in exciton energy transfer and exciton-exciton annihilation, must be explicitly taken into account.^{36,37} For comparison, assuming that a pump photon energy is 3 eV, then 3×10^{12} excitations per cm^2 would correspond to the lasing threshold energy density of $E_{th} \sim 1 \mu\text{J cm}^{-2}$, which is two orders of magnitude lower than demonstrated for organic VCSELs, to date.³⁸ Note that a high peak pump power ($\sim 1 \text{ MW cm}^{-2}$) would be required for exciting the exciton-

polariton laser, with even higher power needed than for organic VCSELs, owing to the short photon lifetime of $\tau \sim 1 \text{ ps}$ in the cavity.³⁹ The short cavity photon lifetime also governs the excited state lifetime of exciton polaritons, which inhibits their diffusion, and inadvertent polariton-polariton annihilation.

In conclusion, we demonstrated intracavity optical pumping of exciton polaritons in J-aggregate microcavity systems using a luminescent cavity spacer layer and show that the occupation of the lower-branch exciton polaritons in such a system at room temperature is thermalized, with relative occupation following a Maxwell-Boltzmann distribution at $T = 300 \text{ K}$. We suggest that a type of “polariton laser” could be fabricated in organic systems by making a VCSEL whose gain material is the luminescent cavity spacer layer and which lases in a strongly coupled exciton-polariton mode.

M.S.B. acknowledges the support of the Department of Defense. The work was supported by the U.S. Department of Energy, Office of Basic Energy Sciences as part of the MIT Energy Frontier Research Center on Excitonics.

*bulovic@mit.edu

- ¹D. G. Lidzey, D. D. C. Bradley, M. S. Skolnick, T. Virgili, S. Walker, and D. M. Whittaker, *Nature (London)* **395**, 53 (1998).
- ²D. G. Lidzey, D. D. C. Bradley, T. Virgili, A. Armitage, M. S. Skolnick, and S. Walker, *Phys. Rev. Lett.* **82**, 3316 (1999).
- ³J. R. Tischler, M. S. Bradley, Q. Zhang, T. Atay, A. Nurmikko, and V. Bulovic, *Org. Electron.* **8**, 94 (2007).
- ⁴R. J. Holmes and S. R. Forrest, *Org. Electron.* **8**, 77 (2007).
- ⁵J. R. Tischler, M. S. Bradley, V. Bulovic, J. H. Song, and A. Nurmikko, *Phys. Rev. Lett.* **95**, 036401 (2005).
- ⁶J. Kasprzak *et al.*, *Nature (London)* **443**, 409 (2006).
- ⁷S. Utsunomiya, L. Tian, G. Roumpos, C. W. Lai, N. Kumada, T. Fujisawa, M. Kuwata-Gonokami, A. Löffler, S. Hoffing, A. Forchel, and Y. Yamamoto, *Nat. Phys.* **4**, 700 (2008).
- ⁸A. Amo, *et al.*, *Nature (London)* **457**, 291 (2009).
- ⁹H. Deng, H. Haug, and Y. Yamamoto, *Rev. Mod. Phys.* **82**, 1489 (2010).
- ¹⁰S. Kéna-Cohen and S. R. Forrest, *Nat. Photonics* **4**, 371 (2010).
- ¹¹F. Tassone, C. Piermarocchi, V. Savona, A. Quattropani, and P. Schwendimann, *Phys. Rev. B* **56**, 7554 (1997).
- ¹²F. Stokker-Cheregi, A. Vinattieri, F. Semond, M. Leroux, I. R. Sellers, J. Massies, D. Solnyshkov, G. Malpuech, M. Colocci, and M. Gurioli, *Appl. Phys. Lett.* **92**, 042119 (2008).
- ¹³J. Chovan, I. E. Perakis, S. Ceccarelli, and D. G. Lidzey, *Phys. Rev. B* **78**, 045320 (2008).
- ¹⁴V. M. Agranovich, M. Litinskaia, and D. G. Lidzey, *Phys. Status Solidi B* **234**, 130 (2002).
- ¹⁵M. Litinskaya, P. Reineker, and V. M. Agranovich, *Phys. Status Solidi A* **201**, 646 (2004).
- ¹⁶P. Michetti and G. L. Rocca, *Phys. Rev. B* **71**, 115320 (2005).
- ¹⁷M. Litinskaya, *Phys. Lett. A* **372**, 3898 (2008).
- ¹⁸M. Litinskaya and P. Reineker, *Phys. Rev. B* **74**, 165320 (2006).
- ¹⁹D. Solnyshkov, H. Ouerdane, M. Glazov, I. Shelykh, and G. Malpuech, *Solid State Commun.* **144**, 390 (2007).
- ²⁰M. Litinskaya, P. Reineker, and V. Agranovich, *J. Lumin.* **110**, 364 (2004).
- ²¹M. Litinskaya, P. Reineker, and V. Agranovich, *J. Lumin.* **119-120**, 277 (2006).
- ²²P. Michetti and G. C. La Rocca, *Phys. Rev. B* **77**, 195301 (2008).
- ²³P. Michetti and G. C. La Rocca, *Phys. Rev. B* **79**, 035325 (2009).
- ²⁴L. Mazza, L. Fontanesi, and G. C. La Rocca, *Phys. Rev. B* **80**, 235314 (2009).
- ²⁵J. Cho, K. Char, J.-D. Hong, and K.-B. Lee, *Adv. Mater.* **13**, 1076 (2001).
- ²⁶P. A. Chiarelli *et al.*, *Adv. Mater.* **13**, 1167 (2001).
- ²⁷V. E. Campbell, P. A. Chiarelli, S. Kaur, and M. S. Johal, *Chem. Mater.* **17**, 186 (2005).
- ²⁸J. Park, L. D. Fouché, and P. T. Hammond, *Adv. Mater.* **17**, 2575 (2005).
- ²⁹M. S. Bradley, J. R. Tischler, and V. Bulovic, *Adv. Mater.* **17**, 1881 (2005).
- ³⁰A. Kavokin, J. J. Baumberg, G. Malpuech, and F. P. Laussy, *Microcavities* (Oxford University Press, Oxford, 2007).
- ³¹M. Litinskaya and P. Reineker, *J. Lumin.* **122-123**, 418 (2007).
- ³²F. M. Marchetti, M. H. Szymanska, P. R. Eastham, B. D. Simons, and P. B. Littlewood, *Solid State Commun.* **134**, 111 (2005).
- ³³G. Christmann, R. Butte, E. Feltin, J. F. Carlin, and N. Grandjean, *Phys. Rev. B* **73**, 153305 (2006).
- ³⁴S. Christopoulos *et al.*, *Phys. Rev. Lett.* **98**, 126405 (2007).
- ³⁵D. Solnyshkov, H. Ouerdane, and G. Malpuech, *J. Appl. Phys.* **103**, 016101 (2008).
- ³⁶A. A. Shoustikov, Y. You, and M. E. Thompson, *IEEE J. Sel. Top. Quantum Electron.* **4**, 3 (1998).
- ³⁷J. Mei, M. S. Bradley, and V. Bulovic, *Phys. Rev. B* **79**, 235205 (2009).
- ³⁸V. Bulović, V. G. Kozlov, V. B. Khalfin, and S. R. Forrest, *Science* **279**, 553 (1998).
- ³⁹V. G. Kozlov *et al.*, *J. Appl. Phys.* **84**, 4096 (1998).